Temperature-dependent conductance of deformable molecular devices

Balázs Dóra[1,*] and András Halbritter[2]
[1]*Max-Planck-Institut für Physik komplexer Systeme, Nöthnitzer Str. 38, 01187 Dresden, Germany*
[2]*Department of Physics, Budapest University of Technology and Economics and Condensed Matter Research Group of the Hungarian Academy of Sciences, Budafoki út 8, 1111 Budapest, Hungary*
(Received 26 August 2009; published 1 October 2009)

Transport through a molecular device coupled to a vibrational mode is studied. By mapping it to the Yu-Anderson model in the large contact broadening limit, the zero-bias electric and heat conductances are evaluated nonperturbatively. These exhibit a step from their $T=0$ value to half of its value as T increases due to the opening of the inelastic scattering channel. The spectral function exhibits the Franck-Condon suppressed multiphonon steps. The Wiedemann-Franz law is satisfied at low and high temperatures, but is violated in between. Relations to experiments are discussed.

DOI: 10.1103/PhysRevB.80.155402 PACS number(s): 73.23.−b, 71.38.−k, 73.63.−b, 85.65.+h

I. MOTIVATION

Molecular electronic devices are based on electron transport through individual molecules and have been proposed for many years as possible candidates for future nanoelectronic circuit elements.[1,2] They triggered intense research due to the fundamental challenge of quantum transport in nanoscale systems and by the possibility of tailoring molecular scale structures.[3,4] One of their most appealing features is the importance of local Coulomb interaction between quasiparticles and scattering off local vibrational modes (VMs), which are more pronounced due to the less effective screening mechanisms at small length scales.

A wide range of characterization methods have been developed for collecting information about the microscopic properties of the molecular junctions and probing its excited states, including conductance histogram techniques;[5] Coulomb blockade,[6,7] conductance fluctuation,[8] shot noise,[9] or superconducting subgap structure[10] measurements, operating mainly at low temperatures. An especially important information about molecular junctions is the study of VMs with point-contact or inelastic electron tunneling spectroscopy,[8,11] where the low-temperature zero-bias conductance of the device is perturbed by the excitation of molecular vibrations with an appropriate bias voltage. Indeed, experiments on single molecular devices including fullerenes,[6,7] carbon nanotubes,[12] benzene,[13] and simple molecules (H_2,CO,H_2O) connecting metallic electrodes,[8,11] have revealed the influence of vibrational degrees of freedom supplemented by theoretical simulations of the VMs.[4,14–20]

Whereas the above low-temperature techniques provide a large amount of information about the ground-state properties of the device and small perturbations due to the excitations of the inelastic degrees of freedom, any room-temperature application requires the knowledge of the temperature sensitivity of the device[2] and the impact of the strongly enhanced inelastic scattering processes should be considered.[3]

Moreover, transport through local VMs parallels closely to the Kondo effect.[21] At low/high temperatures, the former comprises a polaronic cloud made of a quantum/classical oscillator, which corresponds to the Kondo singlet/free classical spin in the latter, and the crossover between low and high T is followed by the universal temperature dependent conductivity obtained by nonperturbative methods, in close analogy with the Kondo effect.[22] This can be of intrinsic importance for magnetically robust Kondo-like behavior (or charge Kondo effect)[23] since VMs couple to the charge sector.

Therefore, in this work, we focus on the temperature-dependent transport through molecular devices by studying the electrical and thermal conductance of a model system with nonperturbative analysis, valid for arbitrary electron-vibron couplings.

II. MODEL AND ITS MAPPING

To model a molecular transport junction, we consider the molecular Hamiltonian as

$$H_{\mathrm{mol}} = g_v Q d^+ d + \frac{P^2}{2m} + \frac{m\omega_0^2}{2} Q^2, \tag{1}$$

describing a single electron level coupled to an Einstein phonon. The level is tunnel coupled to leads as

$$H_0 = \sum_k \varepsilon(k) c_k^+ c_k + \sum_k V_k (c_k^+ d + d^+ c_k) + \epsilon_0 d^+ d, \tag{2}$$

where V_k is the hybridization parameter. The contact broadening is given by $\Delta = \pi \rho_0 \langle V_k^2 \rangle_{FS}$. Let us consider symmetric contacts with noninteracting quasiparticles, in which case it suffices to consider a single effective contact[22] with energy dispersion $\varepsilon(k) = v_F k$ and density of states (DOS) $\rho_0 = 1/2\pi v_F$. First, we diagonalize H_0 and express the molecular Hamiltonian in terms of its eigenfunctions. This is achieved by introducing[24]

$$d = \sum_k \nu_k a_k, \quad c_k = \sum_{k'} \eta_{k,k'} a_{k'}, \tag{3}$$

and

$$\nu_k^2 = \frac{2v_F}{L} \frac{\Delta}{(\varepsilon_k - \epsilon_0)^2 + \Delta^2}, \tag{4}$$

where L is the size of the sample. The explicit form of $\eta_{k,k'}$ is irrelevant for our discussion.[24] From now on, we restrict

our attention to the cases when the broadening by the contacts is such[16] that the DOS of the contact and the device are slowly varying on the scale of the phonon energy ω_0 and temperature T. This is realized in the case $\Delta \gg (T, \omega_0)$ and $\Delta > |\epsilon_0|$, when the junction is represented by a resonant level model, thus $\nu_k \sqrt{L} \approx \bar{\nu} = \sqrt{2 v_F \Delta / (\epsilon_0^2 + \Delta^2)}$ is k independent, which are the basic conditions for the mapping to hold. These are often satisfied under realistic conditions.[16,17] Other cases were studied in Ref. 15, 19, and 20. In terms of the transformation in Eq. (3), the total Hamiltonian $H_0 + H_{\rm mol}$ is rewritten as

$$H = \sum_k \varepsilon(k) a_k^+ a_k + \bar{g} Q \Psi^+(0) \Psi(0) + \frac{P^2}{2m} + \frac{m\omega_0^2}{2} Q^2, \quad (5)$$

where $\bar{g} = \bar{\nu}^2 g_v$ and $\Psi(x) = \Sigma_k \exp(ikx) a_k / \sqrt{L}$. Equation (5) is known as the Yu-Anderson model,[25] describing conduction electrons interacting with a local bosonic mode. The model is solved by bosonizing the fermionic field[21,26] as $\Psi(x) = \exp[i\sqrt{4\pi}\Phi(x)] / \sqrt{2\pi\alpha}$ and the resulting effective model of one-dimensional coupled harmonic oscillators[27] reads as

$$H = v_F \int_{-\infty}^{\infty} dx [\partial_x \Phi(x)]^2 + \frac{g}{\sqrt{\pi}} Q \partial_x \Phi(0) + \frac{P^2}{2m} + \frac{m\omega_0^2}{2} Q^2, \quad (6)$$

where g is the phase shift caused by $\bar{g}$, $\Phi(x)$ stems from the bosonic representation of the fermion field. The VM softens and the damped frequencies are given by[21]

$$\omega_{p\pm} = -i\Gamma \pm \sqrt{\omega_0^2 (1 - \Gamma/\Gamma_2) - \Gamma^2}, \quad (7)$$

where $\Gamma_2 = \pi\omega_0^2 / 4W \ll \omega_0 \ll W$, W is the bandwidth of the conduction electrons, and $\Gamma = \pi (g\rho_0)^2 / 2m$ for small g, and the model becomes unstable for $\Gamma > \Gamma_2$. The explicit dependence of Γ on g_v cannot be determined by the bosonization approach.[21] The $\Gamma < \Gamma_1 \approx \Gamma_2 (1 - \Gamma_2^2 / \omega_0^2)$ region corresponds to underdamped phonons, while the overdamped response shows up at $\Gamma_1 < \Gamma < \Gamma_2$ with two distinct dampings.

III. CONDUCTANCES AT LOW AND HIGH TEMPERATURES

The electric (G) and heat conductance (κ) through the molecular transport junction in the wideband limit are given by[22]

$$\begin{bmatrix} G \\ \kappa \end{bmatrix} = \frac{\Delta}{h} \int d\omega \frac{\partial f}{\partial \omega} \begin{bmatrix} e^2 \\ T\omega^2 \end{bmatrix} \mathrm{Im}\, G_d(\omega), \quad (8)$$

where f is the Fermi function, and $G_d(\omega)$ is Green's function of the electron on the molecule. From Eq. (3),

$$G_d(\omega) = \bar{\nu}^2 G_\Psi(\omega) \quad (9)$$

at $x=0$. This basic relation allows us to determine the properties of localized electron from the Yu-Anderson model. At $T=0$, one can derive a Fermi-liquid relation for the Green's function of the Ψ field[19,28] at $x=0$ as

$$G_\Psi(\omega = 0) = -i\pi\rho_0, \quad (10)$$

which holds true even in the presence of VMs, i.e., the zero-temperature zero-frequency density of states remains unchanged. This occurs because at $T=0$, the incoming electrons experience a frozen Fermi see and no bosons in the oscillator, thus no phase space for scattering. Identical results are obtained for the Kondo model. This leads to the conductance at $T=0$ as

$$G(T=0) = \frac{e^2}{h} \frac{\Delta^2}{\Delta^2 + \epsilon_0^2}, \quad (11)$$

which ranges from perfect transmission ($G(0) = e^2/h$) for $|\epsilon_0| \ll \Delta$ to a decent suppression of the conductance to $\sim 0.7 - 0.8 e^2/h$ for $|\epsilon_0| \lesssim \Delta$. Equation (11) is expected to hold for low transparency junctions, beyond the validity of our mapping as well. The heat conductance satisfies

$$\lim_{T\to 0} \frac{\kappa(T)}{T} = L_0 G(T=0), \quad (12)$$

where $L_0 = (\pi k_B / e)^2 / 3$ is the Lorentz number, thus the Wiedemann-Franz law is fulfilled. At high temperatures ($T > \max(|\omega_{p\pm}|, |\omega_{p+}\omega_{p-}|/\Gamma)$, but still obeying to $T \ll \Delta$, the $\mathcal{T}$ matrix for the Ψ field reaches its universal value, $\mathcal{T} = 1/i2\pi\rho_0$. This halves the corresponding Green's function at $x=0$ in this high T region as

$$G_\Psi(\omega) = G_\Psi^0 + G_\Psi^0 \mathcal{T} G_\Psi^0 = -\frac{i\pi\rho_0}{2} \quad (13)$$

with $G_\Psi^0 = -i\pi\rho_0$, which determines the conductance at high temperatures as

$$G(T \gg \omega_0) = \frac{G(T=0)}{2}. \quad (14)$$

The phonon state is populated by many bosons at high temperatures and every incoming electron scatters off them inelastically with increasing probability even in the weak-coupling limit. The inelastic scattering cross-section reaches its maximal value[28] at this temperature range for arbitrary electron-vibration coupling. The electrons dephase completely and can scatter forward and backward with equal probability ($=1/2$). Consequently, the $\mathcal{T}$ matrix takes the above universal value, and the conductance halves. Similar conclusions about halving the spectral weight were reached for scattering on a dynamical boundary condition.[29]

In the above high T limit, the heat conductance also satisfies $\kappa(T \gg \omega_0)/T = \frac{\pi^2}{3e^2} G(T \gg \omega_0)$, and the Wiedemann-Franz law holds. Therefore, both the electric and heat conductances are expected to exhibit a step from their $T=0$ value to half of its value with increasing temperatures, and the Wiedemann-Franz law holds in the two limits. In between the two limits, G and κ follows a different temperature dependence: the heat conductance drops faster with the temperature and their ratio stays below the universal Lorentz number, hence, the Wiedemann-Franz law is violated, as is shown in Fig. 1. The minimum of their ratio occurs roughly at $3T = \mathrm{Re}\, \omega_{p\pm}$, which can be used as a rule of thumb to estimate the value of the renormalized phonon frequency. We mention that by further increasing the temperature to leave the $T \ll \Delta$ regime, Eq. (1) practically decouples from the conduction electrons. In this regime, the conductances exhibit a second step to zero.

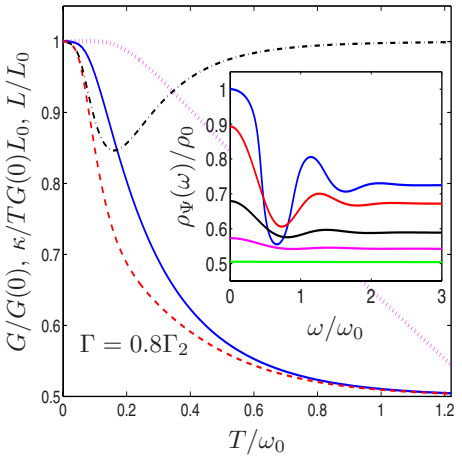

FIG. 1. (Color online) The electric and heat conductance (blue solid and red dashed line) through a molecular junction and their ratio (black dashed-dotted line) is shown as a function of the temperature for $\Gamma=0.8\Gamma_2$, $W=10\omega_0 \Rightarrow \omega_\pm/\omega_0=\pm 0.44-i0.06$, the result of LOPT for the electric conductance (dotted magenta line) is plotted for comparison. The high ($T \gg \mathrm{Re}\,\omega_{p\pm}$) and low ($T \ll \mathrm{Re}\,\omega_{p\pm}$) temperature parts are universal. The inset shows the evolution of the spectral function, $\rho_\Psi(\omega)=-\mathrm{Im}\,G_\Psi(\omega)/\pi$ for $T/\omega_0=0$, 0.2, 0.4, 0.6, and 1.2 from top to bottom.

IV. GREEN'S FUNCTION FROM BOSONIZATION

To study the crossover between the high- and zero-temperature limits, we use the exact result for the Yu-Anderson model obtained from bosonization[21,28] valid for arbitrary temperatures, whose derivation is sketched below. From Eq. (9), the electron Green's function on the molecule is related to that of the Ψ field. The real-time dependence of the latter at the impurity site is obtained in the Yu-Anderson model as

$$G_\Psi(t) = -i\frac{\Theta(t)}{4}\sum_{\gamma,\gamma'=\pm}\lim_{x,y\to 0^+}\langle\{\Psi(\gamma x,t),\Psi^+(\gamma' y,0)\}\rangle$$
$$= -i\frac{\Theta(t)}{8\pi}\sum_{\gamma,\gamma'=\pm}(\exp[C_{\gamma,\gamma'}(t)]+\exp[C_{\gamma',\gamma}(-t)]), \tag{15}$$

Where $C_{\gamma,\gamma'}(t)=\lim_{x,y\to 0^+}4\pi\langle\Phi(\gamma x,t)\Phi(\gamma' y,0)-[\Phi(\gamma x,t)^2+\Phi(\gamma' y,0)^2]/2\rangle-\ln(\alpha)$ and $\alpha\sim 1/W$ is the short distance cutoff in the bosonized theory, γ and γ' denotes the sign of the spatial coordinates x and y. The expectation value $C_{\gamma,\gamma'}(t)$ at bosonic Matsubara frequencies can be evaluated from the bosonized Hamiltonian, Eq. (6) as

$$C_{\gamma,\gamma'}(\omega_m) = -\frac{1}{4|\omega_m|}+\frac{\Gamma}{2}\frac{[\mathrm{sgn}(\omega_m)+\gamma][\mathrm{sgn}(\omega_m)-\gamma']}{(|\omega_m|+i\omega_{p+})(|\omega_m|+i\omega_{p-})}, \tag{16}$$

where $\omega_m=2m\pi T$. The first term is responsible for the $1/t$ decay of the local fermionic propagator, while the second one stems from the interaction of electrons with the oscillator. For $\gamma=\gamma'$, this correction term vanishes. $C_{\gamma,\gamma'}(t)$ is evaluated by analytically continuing the Matsubara frequencies to real ones in Eq. (16), which defines the spectral intensity, and then following Ref. 30, we arrive to the desired correlator. By defining the integral,

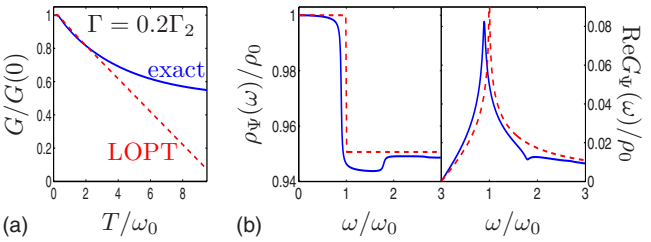

FIG. 2. (Color online) The electric conductance from bosonization (blue solid) and from LOPT (red dashed line) is shown in the left panel as a function of the temperature for weak electron-vibration coupling $\Gamma=0.2\Gamma_2$, $W=10\omega_0 \Rightarrow \omega_\pm/\omega_0=\pm 0.89-i0.02$, signaling the limitations of the LOPT. The deviations grow with the coupling. The right panel shows the real and imaginary part of the Green's function together with the LOPT result at $T=0$.

$$A(t) = \int_{-\infty}^{\infty} d\omega \frac{-i\exp(-i\omega t)}{1-\exp(-\omega/T)}\frac{4\Gamma}{(\omega-\omega_{p+})(\omega-\omega_{p-})}, \tag{17}$$

which follows the derivation of the position autocorrelator of a harmonic oscillator coupled to a heat bath,[27] and can be evaluated in closed form using the hypergeometric functions, the local retarded Green's function at finite temperatures follows as

$$G_\Psi(\omega,T) = -i\pi\frac{\rho_0}{2}\{1+I_{ph}(\omega,T)+\exp[A(0)]\}, \tag{18}$$

where

$$I_{ph}(\omega,T) = \int_0^\infty dt\frac{T\exp(i\omega t)}{\sinh(\pi T t)}\mathrm{Im}\exp[A(t)], \tag{19}$$

whose $T=0$ limit was analyzed in Ref. 28, giving $\mathrm{Im}\,G_\Psi=-i\pi\rho_0$ at $T=\omega=0$. In the $T \gg |\omega_{p+}\omega_{p-}|/\Gamma$ limit, I_{ph} vanishes, and the imaginary part of the propagator is $\mathrm{Im}\,G_\Psi=-i\pi\rho_0/2$, which is the desired result. Plugging Eq. (18) and (9), the conductances are evaluated from Eq. (8), which are shown in Fig. 1 for the full T range, which agree nicely with the analysis of limiting cases. The inset shows the local spectral function, the Franck-Condon steps[14,15] arising from multivibron excitations are smooth due to the significant phonon damping. Notice its explicit temperature dependence through the phonon occupation number. The power of the exact solution manifests itself in comparison with lowest-order perturbation theory (LOPT),[18,31] which neglects multiphonon contributions (becoming dominant with temperature), frequency renormalization and lifetime effects, as is visualized in Fig. 2. LOPT predicts

$$\frac{\rho_\Psi(\omega)}{\rho_0} = 1-\frac{\Gamma\pi}{\omega_0}\left[\coth\left(\frac{\omega_0}{2T}\right)+\sum_{s=\pm} sf(\omega+s\omega_0)\right], \tag{20}$$

which breaks down completely at $T \gg (\omega_0, \omega_0^2/\Gamma)$ even in the weak-coupling regime, leading to the complete suppression and even a sign change in G at high temperatures. The short-

coming of LOPT is even more compelling for stronger couplings, as is shown in Fig. 1.

V. DISCUSSION

Experimentally, the renormalized vibration frequency is determined from the current-voltage characteristics: the dI/dV exhibits a step down in the large contact broadening limit[18] at $eV=\mathrm{Re}\,\omega_{p\pm}$, which sets the characteristic temperature range of the predicted conductance change. As a very rough estimate, the $T=0$ conductance is $\sim\rho_f(\omega\to eV)$, showing the multiphonon structures with the Franck-Condon suppression[14] in the inset of Figs. 1 and 2. We mention that low transmission junctions exhibit a step up in both the out-of-equilibrium dI/dV and the equilibrium spectral function at the excitation of the first VM. Temperature-dependent transport is feasible on molecular devices,[32] albeit large temperature variations are often accompanied by structural changes or the mechanical deformation of the junction. Therefore, the basic ingredients for the observation of the predicted conductance step are the extreme mechanical stability of the device and a low enough frequency ($\mathrm{Re}\,\omega_{p\pm}$) of the VM. Fullerenes like C_{60} were found[6] to possess a center-of-mass oscillation of 50 K, which can be lowered by considering heavier members of their family (e.g., C_{140}). In this case, the oscillation frequency can accurately be estimated based on the interactions (electrostatic, van der Waals) between the molecule and the electrodes. In addition, the intercage VMs of C_{140} start from 25 K.[7] Another promising configuration using a suspended quantum dot phonon cavity,[33] possesses a vibrational frequency of 0.8 K. The actual temperature where the conductance halves, is estimated from Figs. 1 and 2 as $T\sim(2-20)\times\mathrm{Re}\,\omega_{p\pm}$ (the frequency at which a structure shows up in dI/dV), depending on the strength of the electron-vibron coupling.

Although the electron-vibration coupling (g_v) is hardly controllable, the parameters Δ and ρ_0 can be tuned by varying the contact DOS or by gate electrode,[34] which can drive the system toward stronger effective couplings. This decreases the temperature window for the conductance step. Given a low vibrational frequency, condition $\Delta\gg(T,\omega_0)$ is easily met, therefore we expect that a dedicated setup allows the observation of the universal conductance steps, while low-temperature dI/dV measurements can reveal the multiphonon structures in the local spectral function on the molecule. Even for molecular devices, where the direct temperature dependence cannot be traced, our results demonstrate the role of multiphonon scattering processes in the room-temperature conductance of the junction. Our results apply to the electric and heat transport of a metal with dilute concentration of heavy nonmagnetic impurities (with a low vibrational frequency) as well.

In summary, we studied nonperturbatively the electric and heat conductance through a single level coupled to a VM by mapping it to the Yu-Anderson model. With increasing temperature, the conductances drop to half of their $T=0$ value due to increasing inelastic scattering in the large contact broadening limit. We argue that its experimental observation is within reach in stable contacts with a low VM.

ACKNOWLEDGMENTS

This work was supported by the Hungarian Scientific Research Funds under Grants No. K72613 and No. K76010 and by the Bolyai program of the Hungarian Academy of Sciences.

*dora@pks.mpg.de

[1] M. A. Reed, C. Zhou, C. J. M. T. P. Burgin, and J. M. Tour, Science **278**, 252 (1997).
[2] A. Nitzan and M. A. Ratner, Science **300**, 1384 (2003).
[3] G. Cuniberti, G. Fagas, and K. Richter, *Introducing Molecular Electronics* (Springer, Berlin, 2005).
[4] M. Galperin, M. A. Ratner, and A. Nitzan, J. Phys.: Condens. Matter **19**, 103201 (2007).
[5] N. Agraït, A. L. Yeyati, and J. M. van Ruitenbeek, Phys. Rep. **377**, 81 (2003).
[6] H. Park, J. Park, A. K. L. Lim, E. H. Anderson, A. P. Alivisatos, and P. L. McEuen, Nature (London) **407**, 57 (2000).
[7] A. N. Pasupathy *et al.*, Nano Lett. **5**, 203 (2005).
[8] R. H. M. Smit, Y. Noat, C. Untiedt, N. D. Lang, M. C. van Hemert, and J. M. van Ruitenbeek, Nature (London) **419**, 906 (2002).
[9] D. Djukic and J. M. van Ruitenbeek, Nano Lett. **6**, 789 (2006).
[10] P. Makk, Sz. Csonka, and A. Halbritter, Phys. Rev. B **78**, 045414 (2008).
[11] O. Tal, M. Krieger, B. Leerink, and J. M. van Ruitenbeek, Phys. Rev. Lett. **100**, 196804 (2008).
[12] B. J. LeRoy, S. G. Lemay, J. Kong, and C. Dekker, Nature (London) **432**, 371 (2004).
[13] M. Kiguchi, O. Tal, S. Wohlthat, F. Pauly, M. Krieger, D. Djukic, J. C. Cuevas, and J. M. van Ruitenbeek, Phys. Rev. Lett. **101**, 046801 (2008).
[14] K. Flensberg, Phys. Rev. B **68**, 205323 (2003).
[15] J. Koch and F. von Oppen, Phys. Rev. Lett. **94**, 206804 (2005).
[16] M. Paulsson, T. Frederiksen, and M. Brandbyge, Phys. Rev. B **72**, 201101(R) (2005).
[17] L. de la Vega, A. Martín-Rodero, N. Agraït, and A. Levy Yeyati, Phys. Rev. B **73**, 075428 (2006).
[18] R. Egger and A. O. Gogolin, Phys. Rev. B **77**, 113405 (2008).
[19] P. S. Cornaglia, D. R. Grempel, and H. Ness, Phys. Rev. B **71**, 075320 (2005).
[20] Z.-Z. Chen, R. Lü, and B.-f. Zhu, Phys. Rev. B **71**, 165324 (2005).
[21] B. Dóra, Phys. Rev. B **75**, 245113 (2007).
[22] D. Giuliano, A. Naddeo, and A. Tagliacozzo, J. Phys.: Condens. Matter **16**, S1453 (2004).
[23] F. D. M. Haldane, Phys. Rev. B **15**, 281 (1977).
[24] G. D. Mahan, *Many Particle Physics* (Plenum Publishers, New York, 1990).
[25] C. C. Yu and P. W. Anderson, Phys. Rev. B **29**, 6165 (1984).
[26] J. von Delft and H. Schoeller, Ann. Phys. **7**, 225 (1998).
[27] U. Weiss, *Quantum Dissipative Systems* (World Scientific, Sin-

gapore, 2000).
[28] B. Dóra and M. Gulácsi, Phys. Rev. B **78**, 165111 (2008).
[29] M. Fuentes, A. Lopez, E. Fradkin, and E. Moreno, Nucl. Phys. B **450**, 603 (1995).
[30] D. N. Zubarev, Sov. Phys. Usp. **3**, 320 (1960).
[31] S. Engelsberg and J. R. Schrieffer, Phys. Rev. **131**, 993 (1963).
[32] J. J. Parks, A. R. Champagne, G. R. Hutchison, S. Flores-Torres, H. D. Abruña, and D. C. Ralph, Phys. Rev. Lett. **99**, 026601 (2007).
[33] E. M. Weig, R. H. Blick, T. Brandes, J. Kirschbaum, W. Wegscheider, M. Bichler, and J. P. Kotthaus, Phys. Rev. Lett. **92**, 046804 (2004).
[34] L. H. Yu, Z. K. Keane, J. W. Ciszek, L. Cheng, M. P. Stewart, J. M. Tour, and D. Natelson, Phys. Rev. Lett. **93**, 266802 (2004).